Denier, James Patrick ; Mureithi, E. W.
Weakly nonlinear wave motions in a thermally stratified boundary layer, Journal of Fluid Mechanics, 1996; 315:293-316

J. Fluid Mech. (1996), vol. 315, pp. 293–316



# Weakly nonlinear wave motions in a thermally stratified boundary layer

By JAMES P. DENIER[1] AND EUNICE W. MUREITHI[2]

[1]Department of Applied Mathematics, University of Adelaide, South Australia 5005, Australia
[2]School of Mathematics, University of New South Wales, Sydney 2052, Australia

(Received 17 October 1995 and in revised form December 1995)

We consider weakly nonlinear wave motions in a thermally stratified boundary layer. Attention is focused on the upper branch of the neutral stability curve, corresponding to small wavelengths and large Reynolds number. In this limit the motion is governed by a first harmonic/mean flow interaction theory in which the wave-induced mean flow is of the same order of magnitude as the wave component of the flow. We show that the flow is governed by a system of three coupled partial differential equations which admit finite-amplitude periodic solutions bifurcating from the linear, neutral points.

## 1. Introduction

Classical studies on the stability of Tollmien–Schlichting (TS) waves along the lower and upper branches of the neutral curve have been conducted by Lin (1955), Reid (1965) and Stuart (1963), amongst others. In the case of a neutrally stable TS wave mode the flow develops a critical point at the wall-normal position where the flow speed and the disturbance wavespeed coincide; the linear, inviscid, governing equations develop a logarithmic singularity which must be smoothed out by the re-introduction of viscosity in the vicinity of the critical point.

It was not until the work of Smith (1979*a*) that the effect of non-parallelism on the stability characteristics of TS waves was first fully appreciated. Smith developed a self-consistent asymptotic approach for the study of TS waves, and demonstrated that, in the case of lower-branch TS waves, the flow develops a three-tiered structure, the so-called 'triple deck'. These ideas were later utilized by Smith & Bodoyni (1980) to consider, in part, the stability characteristics of the upper branch of the neutral stability curve. Again, a self-consistent asymptotic approach, employing the fact that the Reynolds number of the flow must necessarily be large in order for a boundary layer to exist, was adopted and the flow was shown to be composed of a set of five distinguishable asymptotic régimes in the wall-normal direction. The major difference between the structure of the upper- and lower-branch modes lies in the fact that for the upper-branch modes the critical layer becomes detached from the wall whereas in the case of the lower branch modes it is confined to the lower deck of the standard triple deck. Furthermore, the stability characteristics of upper-branch TS waves are largely governed by the curvature of the velocity profile (this, in turn, is forced by the external streamwise pressure gradient within the boundary layer). These results, which are applicable to accelerating boundary layer flows forced by an external pressure gradient, were extended to encompass Blasius-type boundary layers

by Bodonyi & Smith (1981). The results of that study demonstrated that, again, upper-branch TS waves are governed by a five-tiered structure and, furthermore, the effect of the inherently non-parallel nature of the boundary layer flow is felt earlier than would be anticipated from a purely parallel, Orr–Sommerfeld-type, calculation (see Drazin & Reid 1981). Thus, for both streaming and non-streaming boundary layer flows, upper- and lower-branch TS waves are governed by a five- or three-tiered 'triple deck' structure, respectively.

The concern of the present work is with nonlinear wave motions within thermally stratified boundary layers and we now turn our attention to a discussion of the modifications required to the standard triple deck structure once the question of thermal stratification is considered. We will confine our attention to a discussion of wave-like disturbances to the boundary layer; the reader is referred to the works of Hall & Morris (1992) and Hall (1993) (and references contained therein) for a discussion of longitudinal vortex instabilities in heated boundary layers.

The effect of thermal stratification on the stability characteristics of lower-branch Tollmien-Schlichting waves has been considered by Gage & Reid (1968), Gage (1971), Strehle (1978) and Mureithi & Denier (1996), for incompressible flows and by Seddougui, Bowles & Smith (1991) for a compressible boundary layer. The work of Gage & Reid (1968) was concerned with the effect of thermal stratification on plane Poiseuille flow. They demonstrated that the curve of neutral stability becomes closed for sufficiently strong stable stratification whereas the region of instability was increased in the case of unstable stratification. The work of Gage (1971) extended the results of Gage & Reid (1968) to consider the effect of stable thermal stratification on boundary layer flows. A similar study was carried out by Strehle (1978). The aforementioned works were posed as an Orr–Sommerfeld eigenvalue problem within the framework of a parallel flow approximation to the basic flow and thus ignored the important effect of the non-parallelism of the underlying basic flow. In particular, their result that the curve of neutral stability becomes closed, as the stable thermal stratification is increased, at a finite Reynolds number is not tenable for a true, non-parallel boundary layer due to the underlying, mutually exclusive, assumptions on the Reynolds number that it be both large (in order for a boundary layer to exist) and an order-one quantity for the Orr–Sommerfeld eigenvalue approach to have meaning. The work of Mureithi & Denier (1996) removed this inconsistency, by posing the stability problem in terms of the triple-deck structure of Smith (1979*a*, *b*), and demonstrated the importance of non-parallelism for both stable and unstable thermally stratified boundary layers. In the case of stable thermal stratification (corresponding to strong wall cooling) the eigenvalue problem governing the stability of the flow is identical to that derived by Mureithi, Denier & Stott (1996) for upper-branch TS modes thus suggesting that the curve of neutral stability will, indeed, become closed for sufficiently large Reynolds numbers. The results of Mureithi & Denier (1996) are not unrelated to the work of Seddougui *et al.* (1991) who considered the effect of wall cooling on the stability properties of compressible boundary layers. Their results demonstrate that wall cooling increases the growth rate of TS waves and, in some instances, renders viscous modes of instability more unstable than the purely inviscid modes of instability also present within compressible flows.

In contrast to the behaviour described above the stability characteristics of a boundary layer which exhibits strong unstable thermal stratification are markedly different. Of particular relevance to the present work is the effect on the upper branch of the curve of neutral stability. Such was the motivation of the work of Mureithi *et al.* (1996) who considered the effect of slowly increasing the level of

thermal stratification on upper-branch TS waves. For mildly stratified, heated, boundary layers the standard five-tiered structure of Smith & Bodoyni (1980) is unaltered; however, as the temperature differential between the flat plate and the free stream is increased so the five-tiered structure requires modification. The leading-order TS eigenrelation is first modified when the buoyancy parameter $G$ (see §2 for a definition) becomes $O(Re^{5/12})$ (where $Re$ is the Reynolds number of the flow). At this order the boundary layer is still only weakly stratified; weak in the sense that the momentum and energy fields within the boundary layer remain decoupled. As the buoyancy parameter is further increased to $O(Re^{1/2})$, so that the energy and momentum fields within the boundary layer become fully coupled, the boundary layer flow is rendered inviscidly unstable, the five-tiered structure collapses to a two-tiered inviscid/viscous structure and the stability properties of the flow are governed by the Taylor–Goldstein equation, Drazin & Reid (1981). The Taylor–Goldstein equation possesses modal solutions in the form of temporally growing waves; the flow is inviscidly unstable over a large component of the wavenumber spectrum and, as a consequence, the upper branch of the curve of neutral stability is pushed into a régime of increasingly short wavelengths (short when compared to the boundary layer thickness). These unstable modes are, however, eventually stabilized by viscosity and the neutral modes are found to be isolated to within a thin viscous layer about the position where the streamwise velocity attains a maximum.

At this point we should note that the streamwise velocity in strongly stratified boundary layers can overshoot its free-stream value and as such must attain a definite maximum somewhere within the boundary layer (see Stewartson 1964 and §2 for further discussion on this point).

The new, viscous, neutral upper-branch modes now have many of the characteristics of short-wavelength Görtler vortices commonly encountered in boundary layer flows over curved surfaces; see the review paper by Hall (1990), and references contained therein, for a detailed discussion of short-wavelength vortex motions. Such short-wavelength vortex modes have the remarkable property that their nonlinear development, both weakly nonlinear vortex motions as considered by Hall (1983) and strongly nonlinear vortex motions as considered by Hall & Lakin (1988), are governed by a first harmonic/mean flow interaction theory in which the vortex-induced mean flow is of the same order of magnitude as the vortex motion. The similarities between the upper-branch neutral modes in strongly stratified boundary layers, described in Mureithi *et al.* (1996), and the right-hand-branch, short-wavelength vortex modes described by Hall (1982) suggests that such a wave/mean flow interaction theory will be relevant to the near-neutral wave modes encountered in heated boundary layers. Such, indeed, is the case as will be demonstrated in the coming sections.

The nonlinear wave structure to be described here is applicable to a wide variety of physically important fluid flows. The only restrictions that are placed on the range of validity of this theory are that, firstly, the streamwise velocity of the flow must posses a maximum within the flow field and, secondly, inviscid wave-like disturbances to the basic flow must be governed by the Taylor–Goldstein equation (see §2). Thus the weakly nonlinear wave interaction theory presented here is applicable (after some slight modification) to combined forced–free convection boundary layer flows (over flat, curved and inclined heated plates), heated Poiseuille flow in a channel, mixed heated Poiseuille–Couette flow, Hagen–Poiseuille flow in a heated pipe, as well as many other physically important fluid flows.

Before proceeding with a discussion of nonlinear wave motions within a heated boundary layer, mention should be made of the pioneering work of Benney & Chow

(1985, 1986, 1989) (and references contained therein) on mean flow/first harmonic theories of hydrodynamic stability. Although it is not clear from this analysis that the wave motions they consider are neutrally stable, thus making their results somewhat flawed, they do, however, embody most of the ideas to be found in subsequent wave/mean flow interaction theories and are therefore relevant to the present study.

In this paper we adopt the following structure. In §2 we formulate the problem of weakly nonlinear wave motions within a thermally stratified boundary layer by deriving the characteristic length and time scales of the disturbance as well as the wave amplitude at which nonlinearity will first, significantly, alter the stability characteristics of the flow. In §3 we show that the perturbation wave amplitude, wave-induced mean velocity and mean temperature are governed by a system of three nonlinear coupled partial differential equations. In §§4–6 finite-amplitude periodic solutions of these equations will be described: numerically in §4, in the small-amplitude limit in §5 and the large-amplitude limit in §6. Finally in §7 we draw some conclusions from the present work.

## 2. Formulation of the problem

The non-dimensional form of the equations governing a two-dimensional incompressible fluid flowing over a heated flat plate are, under the Boussinesq approximation, given by

$$\left.\begin{aligned}
&\frac{\partial \tilde{u}}{\partial x}+\frac{\partial \tilde{v}}{\partial y}=0,\\
&\frac{\partial \tilde{u}}{\partial t}+\tilde{u}\frac{\partial \tilde{u}}{\partial x}+\tilde{v}\frac{\partial \tilde{u}}{\partial y}=-\frac{\partial \tilde{p}}{\partial x}+\frac{1}{Re}\nabla^2\tilde{u},\\
&\frac{\partial \tilde{v}}{\partial t}+\tilde{u}\frac{\partial \tilde{v}}{\partial x}+\tilde{v}\frac{\partial \tilde{v}}{\partial y}=-\frac{\partial \tilde{p}}{\partial y}-\frac{Lg}{U_\infty^2}(1-\hat{\alpha}(T_\infty-T_0))+G\tilde{T}+\frac{1}{Re}\nabla^2\tilde{v},\\
&\frac{\partial \tilde{T}}{\partial t}+\tilde{u}\frac{\partial \tilde{T}}{\partial x}+\tilde{v}\frac{\partial \tilde{T}}{\partial y}=\frac{1}{PrRe}\nabla^2\tilde{T},
\end{aligned}\right\} \tag{2.1}$$

where

$$\nabla^2=\frac{\partial^2}{\partial x^2}+\frac{\partial^2}{\partial y^2}.$$

Here we have defined $G = GrRe^{-2}$, with $Gr = g\hat{\alpha}L^3(T_0 - T_\infty)/\nu^2$ being the Grashof number, $Pr$ the Prandtl number, $\hat{\alpha}$ the coefficient of volume expansion, $\nu$ the kinematic viscosity and $g$ the acceleration due to gravity. All velocities have been non-dimensionalized by a typical free-stream speed $U_\infty$, distances by a typical length scale $L$, pressure by $\rho_0 U_\infty^2$, time by $L/U_\infty$ and temperature by $T_0 - T_\infty$, where $T_\infty$ is the free-stream temperature and $T_0$ is the temperature of the plate. Here $\rho_0$ is the density at temperature $T_0$ and the Reynolds number $Re$ is defined as $Re = U_\infty L/\nu$.

In the limit of large Reynolds number the flow develops a boundary layer of thickness $O(Re^{-1/2})$ attached to the leading edge of the plate and in the absence of any disturbances the flow is governed by the steady boundary layer equations. Defining the boundary layer variable $Y = Re^{1/2}y$, the velocity, pressure and temperature fields within the boundary layer can be written as

$$(\tilde{u},\tilde{v},\tilde{T},\tilde{p}) = (\overline{u}, Re^{-1/2}\overline{v}, \overline{T}, \overline{p}_0 + Re^{-1/2}G\overline{p}_1) + \cdots,$$

where the pressure $\overline{p}_0 = -u_e^2/2$ has been introduced to account for the presence

of a non-uniform streaming velocity $u_e$ in the far field. The steady boundary layer equations are then given by

$$\left.\begin{aligned} &\frac{\partial \bar{u}}{\partial x}+\frac{\partial \bar{v}}{\partial Y}=0,\\ &\bar{u}\frac{\partial \bar{u}}{\partial x}+\bar{v}\frac{\partial \bar{u}}{\partial Y}=u_e u_{ex}-Re^{-1/2}G\frac{\partial \bar{p}_1}{\partial x}+\frac{\partial^2 \bar{u}}{\partial Y^2},\\ &\frac{\partial \bar{p}_1}{\partial Y}=\bar{T},\\ &\bar{u}\frac{\partial \bar{T}}{\partial x}+\bar{v}\frac{\partial \bar{T}}{\partial Y}=\frac{1}{Pr}\frac{\partial^2 \bar{T}}{\partial Y^2}. \end{aligned}\right\} \tag{2.2}$$

In deriving these equations we have retained the, formally, asymptotically small term $Re^{-1/2}G$ in the streamwise momentum equation; we will subsequently confine our attention to the case when this so-called 'buoyancy' parameter is an $O(1)$ quantity (i.e. to the case when $G = O(Re^{1/2})$).

For $O(1)$ values of the parameter $G$ the momentum and temperature fields within the boundary layer are decoupled and the temperature field plays an essentially passive role in determining the motion within the boundary layer. In this case the neutral stability properties of the boundary layer, with respect to Tollmien–Schlichting waves, are most readily described in a self-consistent manner in terms of a triple-deck structure (in the case of the lower branch of the curve of neutral stability) or a multi-(five)-layered structure (in the case of the upper branch of the curve of neutral stability). The reader is referred to the work of Bodonyi & Smith (1981), Lin (1955), Smith (1979*a*, *b*), Smith & Bodoyni (1980, 1982) (and references contained therein) for full details of the asymptotic structures of the upper and lower branches of the neutral curve. As the parameter $G$ is increased the standard multi-layered structures of the upper and lower branches of the curve of neutral stability must be modified to account for the subsequent change in the characteristic length scale of the disturbance. These modifications have recently been described by Mureithi *et al.* (1996), for the case of the upper branch of the neutral curve, and Mureithi & Denier (1996), for the case of the lower branch of the neutral curve (the reader is referred to the aforementioned papers for full details; see also Seddoughi *et al.* 1991 for a discussion of wall cooling effects on the triple-deck structure of a compressible boundary layer). At the point when $G = O(Re^{1/2})$, so that the momentum and temperature fields within the boundary layer become fully coupled, the classical upper- and lower-branch structures have been dramatically modified.

The theory to be presented here is applicable to the modified upper-branch structure which arises when $G = O(Re^{1/2})$ and we now focus our attention on that problem. The results of Mureithi *et al.* (1996) demonstrate that the characteristic time and length scales appropriate to the upper branch of the neutral curve are now of the same order as the thickness of the underlying boundary layer, namely $O(Re^{-1/2})$. As such, small-amplitude wave-like disturbances to the boundary layer in the form

$$V_0(Y)\exp\left[\mathrm{i}Re^{1/2}\alpha(x-ct)\right]$$

will be governed by the classical Taylor–Goldstein equation, which in the usual notation is

$$(\bar{u}-c)^2\left(\frac{\partial^2 V_0}{\partial Y^2}-\alpha^2 V_0\right)-\left[(\bar{u}-c)\bar{u}_{YY}-G_0\bar{T}_Y\right]V_0=0. \tag{2.3}$$

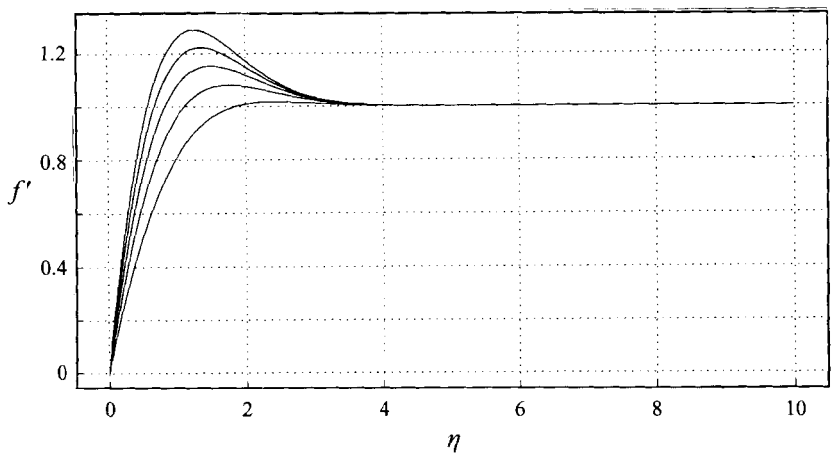


FIGURE 1. Plots of the typical streamwise velocity component for the fully coupled boundary layer equations (2.2). These have been solved in self-similar form by defining $\bar{u} = x^{1/3} f'(\eta)$, $\overline{T} = x^{1/3} g(\eta)$, $\bar{p}_1 = x^{2/3} q(\eta)$ where the similarity variable $\eta = Y/x^{1/3}$. In order to develop such a similarity solution we require the flow to have a free-stream speed $u_e = x^{1/3}$ with a prescribed temperature distribution along the plate given by $T_e = x^{1/3}$. Shown are plots of $f'$ versus $\eta$ for the particular cases $G_0 = GRe^{-1/2} = 1.0, 2.0, 3.0, 4.0, 5.0$.

Here we have set $G_0 = GRe^{-1/2} = O(1)$. For a fixed wavenumber $\alpha$ the disturbance grows or decays with time depending on whether $\mathrm{Im}(c)$ is positive or negative. An important characteristic of the fully coupled boundary layer equations (2.2) which now arises is that the streamwise velocity $\bar{u}$ can develop points of inflexion somewhere in the flow régime. More importantly for the present study is the fact that the flow can develop 'super-velocities'; the streamwise velocity field then attains values greater than those found in the free stream. A typical example is shown in figure 1 where we present a plot of the streamwise velocity, in self-similar form (see the figure caption for details). From this figure we readily observe a finite interval for which $\bar{u} > 1$ (provided of course the buoyancy parameter is of a suitable size). This overshooting of its free-stream value by the streamwise velocity component is a direct consequence of the enhanced acceleration of the fluid due to the effect of thermal buoyancy which manifests itself in the $\bar{p}_1$-component of the pressure. The temperature of the fluid within the boundary layer is a function of both the streamwise and normal coordinates and hence the temperature-induced normal pressure gradient is also a function of both variables. As such, there is now an additional streamwise pressure gradient present in the horizontal momentum equation. Sufficiently far from the heated surface the retarding effect on the fluid by the skin friction will be insufficient to counterbalance the enhanced acceleration of the flow due to the additional pressure component. As such, 'super-velocities' can then be attained in the boundary layer (the reader is referred to Stewartson 1964, §4.3 for further discussion on this point; in particular the occurrence of this effect in compressible boundary layers).

The presence of these super-velocities in the streamwise velocity field ensures that the Taylor–Goldstein equation (2.3) has a full spectrum of temporally growing modes. However, as noted by Mureithi *et al.* (1996), these temporally unstable modes eventually become modified by the effect of viscosity. Indeed, the aforementioned work demonstrated that in the large-wavenumber, $\alpha$, limit the eigensolutions of the Taylor–Goldstein equation have the following properties:

(*a*) the growth rate $\alpha c_i$ approaches a constant in the limit $\alpha \to \infty$;

(*b*) the wave-speed $c_r$ approaches a constant value in the limit $\alpha \to \infty$;

(*c*) the eigenfunction becomes increasingly localized about the location $Y = Y_0$ where the streamwise velocity attains its maximum value. Such a point exists in the present problem due to the presence of the aforementioned 'super-velocities' (see figure 1).

Owing to this spatial localization of the eigenfunction, viscosity must again enter into the equations governing the stability of the boundary layer flow. As such, the instability will no longer be purely inviscid in nature. The results of Mureithi *et al.* (1996) demonstrate that when the wavenumber $\alpha$ achieves size $O(Re^{1/4})$ the disturbance will be confined to an $O(Re^{-3/16})$ viscous layer centred on the position at which $\bar{u}_Y = 0$. Within this wavenumber régime the flow is rendered neutrally stable and its normal structure can be described by a form of the Parabolic Cylinder function equation (see Abramowitz & Stegun 1965).

The characteristic length scales are now $O(Re^{-3/4})$ in the streamwise direction and $O(Re^{-3/16})$ in the direction normal to the plate whilst the new characteristic time scale is $O(Re^{-3/4})$. Let us then define new independent variables $x_1, y_1$ and $T_1$ according to

$$(x_1, y_1, T_1) = (Re^{3/4}x, Re^{3/16}(Y - Y_0), Re^{3/4}t),$$

where $Y = Y_0$ is the position about which the neutral wave modes will be confined. Thus, on the $O(Re^{-3/4})$ time scale, the flow will be neutrally stable; in order for this neutral stability to persist at every order of the expansion we require the wavenumber (with respect to the $x_1$ length scale) and the wavespeed (with respect to the $T_1$ time scale) to expand as

$$(\alpha, c) = (\alpha_{00}, c_{00}) + Re^{-1/8}(\alpha_{01}, c_{01}) + \cdots.$$

The real constants $\alpha_{00}, c_{00}$ etc. are then determined so as to ensure that the flow is neutrally stable and confined to lie within the $O(Re^{-3/16})$ viscous layer (see Mureithi *et al.* 1996 and also §3 for details).

Our concern in this paper is with the effect of nonlinearity on the near-neutral travelling wave modes described above. Assuming, therefore, that the wave motion is confined within an $O(Re^{-3/16})$ viscous layer (centred on the position of maximum streamwise velocity) and has a characteristic length scale $O(Re^{-3/4})$ in the streamwise direction we have, from the Navier–Stokes equations (2.1), the following balance between normal diffusion and nonlinearity:

$$Re^{3/8}\frac{\partial^2 \hat{u}}{\partial y_1^2} \sim Re^{3/4}\hat{u}\frac{\partial \hat{u}}{\partial x_1}, \tag{2.4}$$

where $\hat{u}$ represents the wave amplitude. For nonlinearity to first affect the stability characteristics of the flow, within the viscous sub-layer, we must choose the wave amplitude so that the two terms in (2.4) balance. Therefore, nonlinearity will first affect the neutral stability characteristics of the flow when the wave amplitude is of size $O(Re^{-3/8})$.

## 3. The interaction equations

We are now in a position to write down the reduced equations governing weakly nonlinear wave motions within a thermally stratified boundary layer. In the light of the above discussion we write

$$(\tilde{u}, \tilde{v}, \tilde{T}, \tilde{p}) = (\bar{u}, Re^{-1/2}\bar{v}, \overline{T}, \bar{p}_0 + G_0\bar{p}_1) + Re^{-3/8}(u, Re^{1/16}v, Re^{1/16}\theta, Re^{-1/4}p) + \cdots.$$

Here $\bar{u}, \bar{v}$ are basic boundary-layer velocity components. As we are interested in motions confined within an $O(Re^{-3/16})$ layer, located at the position where $\bar{u}_Y = 0$, we further expand the mean flow quantities as

$$\bar{u} = \bar{u}_0 + \tfrac{1}{2}Re^{-3/8}\bar{u}_2 y_1^2 + \cdots, \qquad \overline{T}_Y = \overline{T}_0 + Re^{-3/16}\overline{T}_1 y_1 + \cdots,$$

where we have defined $\bar{u}_0 = \bar{u}(Y_0), \bar{u}_2 = \bar{u}_{YY}(Y_0), \overline{T}_0 = \overline{T}_Y(Y_0)$ etc. Substituting the above expansions into the Navier–Stokes equations (2.1) yields, after some slight rearrangement,

$$\frac{\partial u}{\partial T_1} + \bar{u}_0\frac{\partial u}{\partial x_1} + Re^{-1/4}\left(\frac{\partial p}{\partial x_1} - \frac{\partial^2 u}{\partial x_1^2}\right) + Re^{-3/8}\left(\frac{\partial u}{\partial T_2} + \frac{1}{2}\bar{u}_2 y_1^2\frac{\partial u}{\partial x_1} + \bar{u}_2 y_1 v - \frac{\partial^2 u}{\partial y_1^2} + u\frac{\partial u}{\partial x_1} + v\frac{\partial u}{\partial y_1}\right) + \cdots = 0, \quad (3.1)$$

$$\frac{\partial v}{\partial T_1} + \bar{u}_0\frac{\partial v}{\partial x_1} + Re^{-1/4}\left(-\frac{\partial^2 v}{\partial x_1^2} - G_0\theta\right) + Re^{-3/8}\left(\frac{\partial v}{\partial T_2} + \frac{1}{2}\bar{u}_2 y_1^2\frac{\partial v}{\partial x_1} + \frac{\partial p}{\partial y_1} - \frac{\partial^2 v}{\partial y_1^2} + u\frac{\partial v}{\partial x_1} + v\frac{\partial v}{\partial y_1}\right) + \cdots = 0, \quad (3.2)$$

$$\frac{\partial \theta}{\partial T_1} + \bar{u}_0\frac{\partial \theta}{\partial x_1} + Re^{-1/4}\left(\bar{T}_0 v - \frac{1}{Pr}\frac{\partial^2\theta}{\partial x_1^2}\right) + Re^{-3/8}\left(\frac{\partial \theta}{\partial T_2} + \frac{1}{2}\bar{u}_2 y_1^2\frac{\partial \theta}{\partial x_1} - \frac{1}{Pr}\frac{\partial^2\theta}{\partial y_1^2} + u\frac{\partial \theta}{\partial x_1} + v\frac{\partial \theta}{\partial y_1}\right) + \cdots = 0, \quad (3.3)$$

$$\frac{\partial u}{\partial x_1} + \frac{\partial v}{\partial y_1} + \cdots = 0, \quad (3.4)$$

where $\cdots$ denotes lower-order terms which will not enter into the subsequent analysis. Here we have introduced the additional time scale $T_2 = Re^{-3/8}T_1$ in order to allow for the slow temporal growth or decay of the wave motion within the flow. In order to solve the system of equations (3.1)–(3.4) we first define

$$E = \exp(i\alpha_0 x_1 - ic_0 T_1) \qquad \text{with} \qquad c_0 = \alpha_0\bar{u}_0,$$

and expand all disturbances in the form (with an asterisk denoting the complex conjugate)

$$u = U_{10}E + U_{m0} + U_{10}^*E^* + Re^{-1/8}(U_{11}E + U_{m1} + U_{11}^*E^* + U_{21}E^2 + U_{21}^*E^{*2}) + \cdots,$$
$$v = V_{10}E + V_{10}^*E^* + Re^{-1/8}(V_{11}E + V_{11}^*E^* + V_{21}E^2 + V_{21}^*E^{*2}) + \cdots,$$
$$\theta = \theta_{10}E + \theta_{m0} + \theta_{10}^*E^* + Re^{-1/8}(\theta_{11}E + \theta_{m1} + \theta_{11}^*E^* + \theta_{21}E^2 + \theta_{21}^*E^{*2}) + \cdots,$$
$$p = Re^{1/8}P_{m0} + (P_{10}E + P_{m1} + P_{10}^*E^*) + Re^{-1/8}(P_{11}E + P_{m2} + P_{11}^*E^* + P_{21}E^2 + P_{21}^*E^{*2}) + \cdots;$$

again $\cdots$ denotes terms which do not enter into the subsequent analysis. Here we have introduced an $O(Re^{1/8})$ mean pressure component in order to balance the $O(1)$ mean temperature component appearing in the expansion for $\theta$. In the above expansion the mean flow terms, denoted by subscripts $mj$, are independent of both $x_1$ and $T_1$. From the equation of continuity, together with the constraint that the motion be confined to within the thin viscous layer centred on $Y = Y_0$, the mean flow component in the vertical direction is found to be identically zero; this fact has been anticipated in the

above expansion. Furthermore, we expand the wavenumber as

$$\alpha_0 = \alpha_{00} + Re^{-1/8}\alpha_{01} + \ldots, \tag{3.5}$$

where $\alpha_{00}$ is the critical wavenumber, to be determined, at which the flow is neutrally stable on the $T_1$ time scale. The additional term $\alpha_{01}$ then determines stability or instability on the $T_2$ time scale. As a consequence of this expansion we have a modification to the leading-order wave speed given by

$$c_0 = \alpha_0\bar{u}_0 = \alpha_{00}\bar{u}_0 + Re^{-1/8}\alpha_{01}\bar{u}_0 + \cdots,$$

where the wave-speed has been chosen such that

$$\left(\frac{\partial}{\partial T_1} + \bar{u}_0\frac{\partial}{\partial x_1}\right)E^n \equiv 0 \qquad \text{for all integers } n.$$

At this point it is worth emphasizing the difference between the nonlinear structure to be derived in the coming sections and the structure which would arise from a standard weakly nonlinear analysis and which would invariably result in a typical Stuart–Landau amplitude equation to describe the temporal development of the wave amplitude. In such a Stuart–Landau approach to weakly nonlinear theory the wave-induced mean flow component would be an order of magnitude smaller than the small amplitude of the wave motion. Thus, for example, if the wave amplitude were taken to be $O(\epsilon)$ (where $\epsilon$ is a small amplitude parameter) then the wave-induced mean flow, which arises through the self-interaction of the wave, would be of $O(\epsilon^2)$. In the present problem the wave amplitude $U_{10}$ and the wave-induced mean flow $U_{m0}$ are of comparable size. Thus, the present analysis could best be described as being fully nonlinear. It is worth noting that the wave/mean flow interaction of the present problem also arises in the context of short-wavelength vortex motions, where the wave component is in the form of a spanwise periodic vortex. It was in this setting that the first, self-consistent, wave/mean flow interaction theory was given by Hall & Lakin (1988) for short-wavelength Görtler vortices within boundary layer flows over concavely curved surfaces. This work has subsequently been extended to many other problems in which the predominant motion is a steady vortex type motion; see Bassom & Hall (1989) and Denier (1992) for two particular examples. The present problem is, however, concerned with unsteady travelling wave solutions of the full Navier–Stokes equations.

To proceed, upon substituting the above expansions into the governing equations (3.1)–(3.4) and equating coefficients of inverse powers of $Re^{1/8}$ we obtain, for the amplitude of the wave-like components,

$$\alpha_{00}^2 V_{10} - G_0\theta_{10} = 0, \tag{3.6}$$

$$\alpha_{00}^2 V_{11} - G_0\theta_{11} = -2\alpha_{00}\alpha_{01}V_{10} - \frac{\partial V_{10}}{\partial T_2} - \frac{\mathrm{i}\alpha_{00}\bar{u}_2 y_1^2}{2}V_{10} - \frac{\partial P_{10}}{\partial y_1} + \frac{\partial^2 V_{10}}{\partial y_1^2} - \mathrm{i}\alpha_{00}U_{m0}V_{10}, \tag{3.7}$$

$$\bar{T}_0 V_{10} + \frac{1}{Pr}\alpha_{00}^2\theta_{10} = 0, \tag{3.8}$$

$$\bar{T}_0 V_{11} + \frac{1}{Pr}\alpha_{00}^2\theta_{11} = -\frac{2\alpha_{00}\alpha_{01}}{Pr}\theta_{10} - \frac{\partial\theta_{10}}{\partial T_2} - \frac{\mathrm{i}\alpha_{00}\bar{u}_2 y_1^2}{2}\theta_{10} + \frac{1}{Pr}\frac{\partial^2\theta_{10}}{\partial y_1^2} - \mathrm{i}\alpha_{00}U_{m0}\theta_{10} - V_{10}\frac{\partial\theta_{m0}}{\partial y_1}, \tag{3.9}$$

$$i\alpha_{00}P_{10} + \alpha_{00}^2 U_{10} = 0, \tag{3.10}$$

$$i\alpha_{00}U_{10} + \frac{\partial V_{10}}{\partial y_1} = 0, \tag{3.11}$$

whereas for the mean flow components we obtain

$$\frac{\partial U_{m0}}{\partial T_2} - \frac{\partial^2 U_{m0}}{\partial y_1^2} = -V_{10}\frac{\partial U_{10}^*}{\partial y_1} - V_{10}^*\frac{\partial U_{10}}{\partial y_1}, \tag{3.12}$$

$$\frac{\partial \theta_{m0}}{\partial T_2} - \frac{1}{Pr}\frac{\partial^2 \theta_{m0}}{\partial y_1^2} = -i\alpha_{00}(\theta_{10}U_{10}^* - \theta_{10}^* U_{10}) - V_{10}\frac{\partial \theta_{10}^*}{\partial y_1} - V_{10}^*\frac{\partial \theta_{10}}{\partial y_1}. \tag{3.13}$$

Equations (3.6) and (3.8) are compatible, that is they yield non-trivial solutions, provided that

$$G_0\bar{T}_0 + \frac{1}{Pr}\alpha_{00}^4 = 0, \tag{3.14}$$

which serves to determine the critical wavenumber $\alpha_{00}$. Note that $\bar{T}_0 < 0$, so that (3.14) yields a real solution for the critical wavenumber

$$\alpha_{00} = \left(PrG_0|\bar{T}_0|\right)^{1/4}.$$

At next order, equations (3.7) and (3.9) are compatible, in the light of (3.14), if

$$\frac{\partial V_{10}}{\partial T_2} - \frac{3}{(1+Pr)}\frac{\partial^2 V_{10}}{\partial y_1^2} + \frac{4\alpha_{00}\alpha_{10}}{(1+Pr)}V_{10} + \frac{i\alpha_{00}\bar{u}_2}{2}y_1^2 V_{10} + i\alpha_{00}U_{m0}V_{10} + \frac{G_0 Pr}{\alpha_{00}^2(1+Pr)}V_{10}\frac{\partial \theta_{m0}}{\partial y_1} = 0. \tag{3.15}$$

Once $V_{10}$ has been determined from (3.15) equations (3.6), (3.10) and (3.11) serve to determine the wave amplitudes $\Theta_{10}$, $P_{10}$ and $U_{10}$ respectively.

At this stage of our analysis the wave-induced mean components $U_{m0}$ and $\theta_{m0}$ remain undetermined. Turning our attention to (3.12) we have, upon making use of continuity as prescribed by (3.11),

$$\frac{\partial U_{m0}}{\partial T_2} - \frac{\partial^2 U_{m0}}{\partial y_1^2} = -\frac{i}{\alpha_{00}}\left(V_{10}^*\frac{\partial^2 V_{10}}{\partial y_1^2} - V_{10}\frac{\partial^2 V_{10}^*}{\partial y_1^2}\right). \tag{3.16}$$

Again making use of (3.11) we have from (3.13)

$$\frac{\partial \theta_{m0}}{\partial T_2} - \frac{1}{Pr}\frac{\partial^2 \theta_{m0}}{\partial y_1^2} = -\frac{2\alpha_{00}^2}{G_0}\frac{\partial}{\partial y_1}|V_{10}|^2. \tag{3.17}$$

Finally rescaling according to

$$\theta_{m0} \to \frac{2\alpha_{00}^2}{G_0}\theta_m, \quad U_{m0} \to \frac{1}{\alpha_{00}}U_m, \quad V_{10} \to V,$$

the system (3.15)–(3.17) can be written as

$$\frac{\partial V}{\partial T_2} = \frac{3}{(1+Pr)}\frac{\partial^2 V}{\partial y_1^2} - \alpha_1 V - ik y_1^2 V - iU_m V - \frac{2Pr}{1+Pr}V\frac{\partial \theta_m}{\partial y_1},$$

$$\frac{\partial U_m}{\partial T_2} = \frac{\partial^2 U_m}{\partial y_1^2} - i\left(V^*\frac{\partial^2 V}{\partial y_1^2} - V\frac{\partial^2 V^*}{\partial y_1^2}\right),$$

$$\frac{\partial \theta_m}{\partial T_2} = \frac{1}{Pr}\frac{\partial^2 \theta_m}{\partial y_1^2} - \frac{\partial}{\partial y_1}|V|^2,$$

where we have defined

$$\alpha_1 = \frac{4\alpha_{00}\alpha_{01}}{(1+Pr)}, \qquad k = \alpha_{00}\bar{u}_2.$$

Note that $k < 0$ since $\bar{u}_2 = \bar{u}_{yy}(Y_0) < 0$. In all that follows we will, for simplicity, take $k = -2, \alpha_{00} = 1$ and $Pr = 2$ (the precise value of these parameters have little quantitative effect on the subsequent analysis). The final form of the equations governing the wave/mean flow interaction are then

$$\frac{\partial V}{\partial T_2} = \frac{\partial^2 V}{\partial y_1^2} - \alpha_1 V + 2\mathrm{i}y_1^2 V - \mathrm{i}U_m V - \frac{4}{3}V\frac{\partial \theta_m}{\partial y_1}, \tag{3.18}$$

$$\frac{\partial U_m}{\partial T_2} = \frac{\partial^2 U_m}{\partial y_1^2} - \mathrm{i}\left(V^*\frac{\partial^2 V}{\partial y_1^2} - V\frac{\partial^2 V^*}{\partial y_1^2}\right), \tag{3.19}$$

$$\frac{\partial \theta_m}{\partial T_2} = \frac{1}{2}\frac{\partial^2 \theta_m}{\partial y_1^2} - \frac{\partial}{\partial y_1}|V|^2. \tag{3.20}$$

This system of equations must be solved subject to the boundary conditions

$$V, U_m, \theta_m \to 0 \quad \text{as} \quad |y_1| \to \infty, \tag{3.21}$$

in order to ensure decay of the motion outside the thin viscous layer situated at $Y = Y_0$, together with suitable initial conditions

$$V = V^0(y_1),\ U_m = U_m^0(y_1),\ \theta_m = \theta_m^0(y_1) \quad \text{at} \quad T_2 = 0.$$

Without resorting to a full numerical solution there seems to be little hope of developing a general solution of the system (3.18)–(3.20). However, in the next section, we will demonstrate the existence of a family of finite-amplitude periodic solutions.

## 4. Periodic solutions

An examination of the system of equations (3.18)–(3.20) suggests the existence of periodic solutions in the form

$$\theta_m = \theta_0(y), \quad U_m = U_0(y), \quad V = V_0(y)\mathrm{e}^{\mathrm{i}\omega T_2},$$

where, for simplicity of notation, we have dropped the subscript on $y_1$. Substitution of these expressions into equations (3.18)–(3.20) yields

$$\frac{\mathrm{d}^2\theta_0}{\mathrm{d}y^2} = 2\frac{\mathrm{d}}{\mathrm{d}y}|V_0|^2, \tag{4.1}$$

$$\frac{\mathrm{d}^2 U_m}{\mathrm{d}y^2} = \mathrm{i}\left(V_0^*\frac{\mathrm{d}^2 V_0}{\mathrm{d}y^2} - V_0\frac{\mathrm{d}^2 V_0^*}{\mathrm{d}y^2}\right), \tag{4.2}$$

$$\frac{\mathrm{d}^2 V_0}{\mathrm{d}y^2} = (\alpha_1 + \mathrm{i}\omega)V_0 - 2\mathrm{i}y^2 V_0 + \mathrm{i}U_0 V_0 + \frac{4}{3}V_0\frac{\mathrm{d}\theta_0}{\mathrm{d}y}. \tag{4.3}$$

Integrating (4.1) and (4.2), and making use of the boundary conditions (3.21), gives

$$\frac{\mathrm{d}\theta_0}{\mathrm{d}y} = 2|V_0|^2, \qquad U_0 = \mathrm{i}\int_y^\infty \left(V_0\frac{\mathrm{d}V_0^*}{\mathrm{d}z} - V_0^*\frac{\mathrm{d}V_0}{\mathrm{d}z}\right)\mathrm{d}z,$$

which, upon substituting into (4.3) yields the nonlinear integro-differential equation

$$\frac{\mathrm{d}^2V_0}{\mathrm{d}y^2} = (\alpha_1 + \mathrm{i}\omega)V_0 - 2\mathrm{i}y^2V_0 - V_0\int_y^\infty \left(V_0\frac{\mathrm{d}V_0^*}{\mathrm{d}z} - V_0^*\frac{\mathrm{d}V_0}{\mathrm{d}z}\right)\mathrm{d}z + \tfrac{8}{3}V_0|V_0|^2. \quad (4.4)$$

Equation (4.4) must be solved subject to the boundary conditions

$$V_0 \to 0 \quad \text{as} \quad |y| \to \infty. \quad (4.5)$$

Before proceeding with a description of our solution methodology for this equation we note that in the limit of infinitesimally small amplitude we obtain the linearized equation

$$\frac{\mathrm{d}^2V_0}{\mathrm{d}y^2} = (\alpha_1 + \mathrm{i}\omega)V_0 - 2\mathrm{i}y^2V_0, \quad (4.6)$$

which is a form of the Parabolic Cylinder function equation whose solutions can be written in the form

$$V_0 = H_m\left(2^{1/4}\mathrm{e}^{-\mathrm{i}\pi/8}y\right)\exp\left\{-(1-\mathrm{i})y^2/2\right\}, \quad (4.7a)$$

where, in order to satisfy the boundary conditions (4.5), we have chosen

$$\alpha_1 + \mathrm{i}\omega = (2m+1)(-1+\mathrm{i}) \qquad (m = 0, 1, 2, \ldots) \quad (4.7b)$$

(here $H_m(z)$ are Hermite polynomials of degree $m$; see Abramowitz & Stegun 1965 for details). There are then an infinite number of eigenmodes satisfying (4.6) and the neutral wavenumbers can now be written as

$$\alpha = \alpha_{00}\left\{1 - Re^{-1/8}\frac{(2m+1)(1+Pr)}{4(PrG_0|\bar{T}_0|)^{1/2}} + \cdots\right\} \qquad (m = 0, 1, 2, \ldots).$$

Thus, along the upper branch of the neutral curve the (un-scaled) streamwise wavenumber expands as, taking $m = 0$ in the above expression,

$$Re^{3/4}(PrG_0|\bar{T}_0|)^{1/4}\left\{1 - Re^{-1/8}\frac{(1+Pr)}{4(PrG_0|\bar{T}_0|)^{1/2}} + \cdots\right\}.$$

For values of the wavenumber less than this critical value the flow is unstable to temporally growing wave modes.

### 4.1. *The numerical scheme*

Turning our attention to the eigenvalue problem posed by (4.4) we define a new dependent variable $A$ according to

$$V_0 = (\bar{A}_0 + \mathrm{i}\bar{B}_0)A.$$

Equation (4.4) can now be rewritten as

$$\frac{\mathrm{d}^2A}{\mathrm{d}y^2} = \sigma A - 2\mathrm{i}y^2A - a^2A\int_y^\infty \left(A\frac{\mathrm{d}A^*}{\mathrm{d}z} - A^*\frac{\mathrm{d}A}{\mathrm{d}z}\right)\mathrm{d}z + \tfrac{8}{3}a^2A|A|^2, \quad (4.8)$$

where we have defined $\sigma = \alpha_1 + \mathrm{i}\omega$ and $a^2 = \bar{A}_0^2 + \bar{B}_0^2$. Noting from (4.1)–(4.3) that the function $V$ can be either odd or even in the normal coordinate $y$ we seek solutions of (4.8) which are either even or odd functions of $y$. Hence the boundary condition

$V_0 \to 0$ as $y \to -\infty$ can be replaced by the boundary condition

$$\frac{\mathrm{d}V_0}{\mathrm{d}y} = 0 \quad \text{on} \quad y = 0 \qquad \text{(for even-mode solutions)}$$

with $V_0(0) = (\bar{A}_0 + \mathrm{i}\bar{B}_0)(1 + \mathrm{i})$ to be determined as part of the solution process, or

$$V_0 = 0 \quad \text{on} \quad y = 0 \qquad \text{(for odd-mode solutions)}$$

with $V_{0y}(0) = (\bar{A}_0 + \mathrm{i}\bar{B}_0)(1 + \mathrm{i})$ to be determined as part of the solution process. The boundary conditions for equation (4.8) can then be written as

$$A = 1 + \mathrm{i}, \ \frac{\mathrm{d}A}{\mathrm{d}y} = 0 \quad \text{on} \quad y = 0, \qquad A \to 0 \quad \text{as} \quad y \to \infty, \tag{4.9}$$

in the case of symmetric solutions, or

$$A = 0, \ \frac{\mathrm{d}A}{\mathrm{d}y} = 1 + \mathrm{i} \quad \text{on} \quad y = 0, \qquad A \to 0 \quad \text{as} \quad y \to \infty, \tag{4.10}$$

in the case of asymmetric solutions. Equation (4.8) together with boundary conditions (4.9) (or their odd counterparts (4.10)) defines an eigenvalue problem for the wavenumber $\alpha_1$ and the frequency $\omega$ as a function of the amplitude $a$. Thus, for a fixed value of the amplitude $a$, we must solve (4.8) subject to the boundary conditions (4.9) on $y = 0$ and determine $\sigma$ such that $A \to 0$ as $y \to \infty$.

In order to achieve this aim the nonlinear integral equation (4.8) was first written as a system of first-order ordinary differential equations with the integral term written in derivative form by defining a new variable $D$ according to

$$\frac{\mathrm{d}D}{\mathrm{d}y} = -\left(A\frac{\mathrm{d}A^*}{\mathrm{d}y} - A^*\frac{\mathrm{d}A}{\mathrm{d}y}\right).$$

The resulting system of equations was solved, for a fixed value of the amplitude $a$, subject to the boundary conditions

$$A = 1 + \mathrm{i}, \quad \text{at} \quad y = 0 \qquad A = 0, \ D = 0 \quad \text{at} \quad y = y_\infty \gg 1 \qquad \text{(for even modes)},$$

$$\frac{\mathrm{d}A}{\mathrm{d}y} = 1 + \mathrm{i} \quad \text{at} \quad y = 0 \qquad A = 0, \ D = 0 \quad \text{at} \quad y = y_\infty \gg 1 \qquad \text{(for odd modes)},$$

using the routine D02RAF from the NAG suite of subroutines. A Newton iteration procedure was then adopted to iterate on the unknowns, namely $\alpha_1$ and $\omega$, until the remaining boundary conditions

$$\frac{\mathrm{d}A}{\mathrm{d}y} = 0 \quad \text{on} \quad y = 0 \qquad \text{(even modes)},$$

or

$$A = 0 \quad \text{on} \quad y = 0 \qquad \text{(odd modes)},$$

were satisfied to within some desired accuracy.

The results of such a calculation are shown in figure 2 in which we present plots of the wavenumber $\alpha_1$ and the frequency $\omega$ versus the amplitude $a$. Shown are the first six modes (three even modes and three odd modes). In all cases we readily observe a bifurcation to a branch of finite-amplitude periodic solutions† as the wavenumber

† We note that we were unable to find any solutions, other than those presented here, to equation (4.8). This does not, of course, preclude the existence of, for example, solutions which are neither odd nor even about the centreline $y = 0$. However the odd and even modes described above are, on the basis of uniqueness of the linear solutions (4.7*a*) of the Parabolic Cylinder function equation,

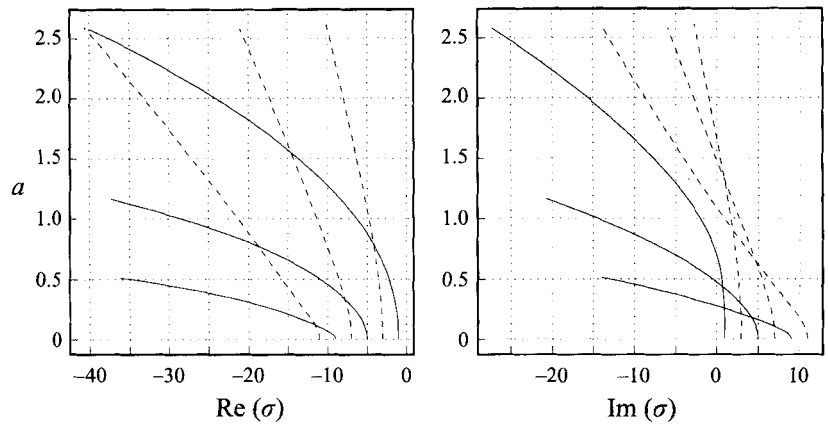


FIGURE 2. The bifurcation diagram for equation (4.8). Here $\alpha_1 = \mathrm{Re}(\sigma)$ and $\omega = \mathrm{Im}(\sigma)$ with even modes (solid lines) and odd modes (dashed).

$\mathrm{Re}(\sigma)$ passes through a succession of bifurcation points, which from (4.7*b*), are located at $\mathrm{Re}(\sigma) = -(2m+1)$ $(m = 0, 1, 2, \ldots)$. The corresponding eigenfunctions for the first four modes are shown in figure 3. We note from figure 3(*c,d,g,h*) that the amplitude of the odd modal solutions decrease with increasing scaled amplitude $a$. This has important implications for the large-amplitude limit of the odd solutions. We will return to this point when we consider the large-amplitude limit in §6.

We are, as yet, unable to determine the stability characteristics of the finite-amplitude bifurcating solutions. In general such a classification requires considerable numerical effort; however, in the limit of small wave amplitude the question of stability can be answered directly by analytic means. Thus, we consider the behaviour of small-amplitude solutions of (4.8), and their stability characteristics, in the next section.

## 5. The small-amplitude limit

### 5.1. *The bifurcating solutions*

In the limit of small amplitude $a$ we can develop a series solution to the bifurcation problem as posed by (4.8) which serves as a useful check on the results of the previous section as well as allowing us to determine the stability properties of the small-amplitude solutions. We expand all quantities in terms of power series in powers of $a^2$. Thus, in the notation of (4.8), we write

$$A = A_0 + a^2 A_1 + a^4 A_2 + \cdots,$$
$$\sigma = \sigma_0 + a^2 \sigma_1 + a^4 \sigma_2 + \cdots.$$

Substitution into (4.8) and equating coefficients of powers of $a^2$ to zero gives

$$\mathscr{L} A_0 = 0, \tag{5.1}$$

$$\mathscr{L} A_1 = \sigma_1 A_0 - A_0 \int_y^\infty \left( A_0 \frac{\mathrm{d}A_0^*}{\mathrm{d}z} - A_0^* \frac{\mathrm{d}A_0}{\mathrm{d}z} \right) \mathrm{d}z + \tfrac{8}{3} A_0 |A_0|^2, \tag{5.2}$$

the only ones which can possibly bifurcate from the linear critical values, given by (4.7*b*), as the amplitude $a$ increases. Thus, if any other solutions were to be found to equation (4.8) they must represent a new family of finite-amplitude solutions.

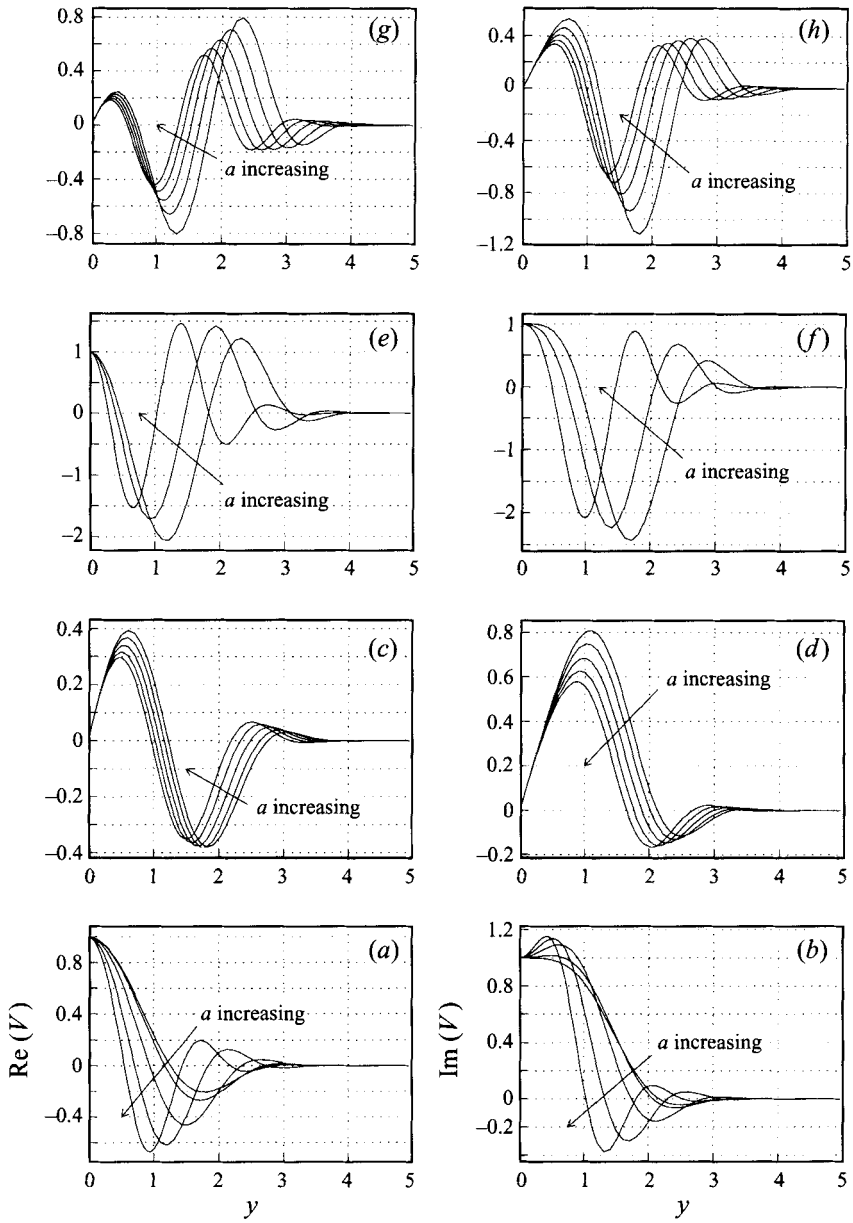


FIGURE 3. Plots of the first four eigenfunctions of equation (4.8). Plots of Re($V$) and Im($V$) for various values of the wave amplitude $a$. Shown are $(a, b)$ mode 1, $(c, d)$ mode 2, $(e, f)$ mode 3, $(g, h)$ mode 4. Plots for increasing amplitude $a$ from $a = 0$ in increments of 0.4.

where we have defined the differential operator $\mathscr{L}$

$$\mathscr{L} = \frac{\mathrm{d}^2}{\mathrm{d}y^2} - \sigma_0 + 2\mathrm{i}y^2.$$

Each of (5.1) and (5.2) must be solved subject to the boundary conditions

$$A_j \to 0 \qquad |y| \to \infty.$$

| Mode number | $A_0/E_1$ | $\sigma_0$ | $\sigma_1/\sqrt{2}$ |
|---|---|---|---|
| 1 | $(1+\mathrm{i})$ | $-1+\mathrm{i}$ | $-4.4415-.8906\mathrm{i}$ |
| 2 | $(1+\mathrm{i})y$ | $-3+3\mathrm{i}$ | $-2.2788-1.5316\mathrm{i}$ |
| 3 | $(1+\mathrm{i})-4y^2$ | $-5+5\mathrm{i}$ | $-28.5056-25.3388\mathrm{i}$ |
| 4 | $[(1+\mathrm{i})-4y^2/3]y$ | $-7+7\mathrm{i}$ | $-8.4226-7.7470\mathrm{i}$ |
| 5 | $(1+\mathrm{i})-8y^2+8(1-\mathrm{i})y^4/3$ | $-9+9\mathrm{i}$ | $-250.3788-217.6518\mathrm{i}$ |
| 6 | $[(1+\mathrm{i})-8y^2/3+8(1-\mathrm{i})y^4/15]y$ | $-11+11\mathrm{i}$ | $-47.6179-37.2625\mathrm{i}$ |

TABLE 1. The leading-order eigenfunctions $A_0$ and the two-term asymptotic expansion of the eigenvalues given by (5.3) and (5.4). Here $E_1=\exp\left(-(1-\mathrm{i})y^2/2\right)$.

Equation (5.1) is readily recognized as the linearized eigenvalue problem which determines the stability of infinitesimally small-amplitude, travelling wave, solutions of the Navier–Stokes equations. Its solution is given by (4.7*a*,*b*). At next order in the expansion equation (5.2) has a solution provided a solvability condition on the right-hand side is satisfied; such a solvability condition is commonly referred to as a Fredholm alternative condition. In order to derive this solvability condition we define an inner product according to

$$\langle v,w\rangle=\int_{-\infty}^{\infty}vw^*\mathrm{d}y.$$

With respect to this inner product the adjoint differential operator $\mathscr{L}^\dagger$ is given by

$$\mathscr{L}^\dagger=\frac{\mathrm{d}^2}{\mathrm{d}y^2}-\sigma_0^*-2\mathrm{i}y^2.$$

The adjoint eigenfunctions, satisfying $\mathscr{L}^\dagger w=0$, are then given by $w=A_0^*$, where $A_0$ is the eigenfunction (4.7*a*). Multiplying (5.2) by $w^*$ and integrating from $-\infty$ to $\infty$ gives

$$0=\sigma_1\int_{-\infty}^{\infty}A_0^2\mathrm{d}y-\int_{-\infty}^{\infty}A_0^2\left(\int_z^{\infty}\left(A_0\frac{\mathrm{d}A_0^*}{\mathrm{d}t}-A_0^*\frac{\mathrm{d}A_0}{\mathrm{d}t}\right)\mathrm{d}t\right)\mathrm{d}z+\frac{8}{3}\int_{-\infty}^{\infty}A_0^2|A_0|^2\,\mathrm{d}y,\quad(5.3)$$

where we have used the fact that $\langle\mathscr{L}A_1,w\rangle=\langle A_1,\mathscr{L}^\dagger w\rangle=0$.

The expression (5.3) now gives the $O(a^2)$ correction to the wavenumber/frequency. We present the results of the calculation of this first-order wavenumber/frequency correction term $\sigma_1$ in table 1, together with the corresponding leading-order eigenfunctions $A_0$. (We note that the eigenfunctions $A_0$ of the linearized operator $\mathscr{L}$ have been chosen so as to satisfy the normalization criteria used in §4, namely that $A_0(0)=1+\mathrm{i}$ for even modes and $A_{0y}(0)=1+\mathrm{i}$ for odd modes). All integrals appearing in (5.3) were evaluated using the algebraic manipulation package Maple.

In figure 4 we present a comparison of the two-term asymptotic expansions for the wavenumber and frequency of the bifurcated solutions, as given in table 1, with the full numerical results obtained in §4. The agreement with the computed results is seen to be good for small to moderate values of the wave amplitude; however, as expected, the results begin to diverge as the amplitude assumes $O(1)$ values.

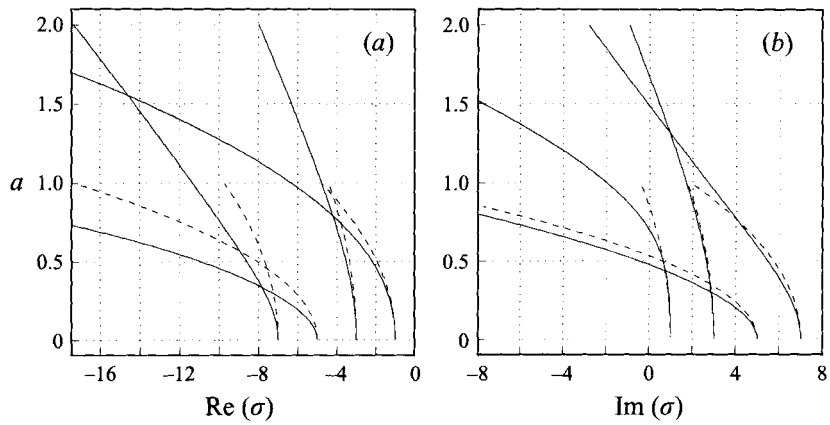


FIGURE 4. Comparison of the two-term, small-amplitude, asymptotic expansion of §5.1 with the numerical results of §4. Shown are (*a*) Re($\sigma$) and (*b*) Im($\sigma$). The dashed curves are the results from the two-term asymptotic expansion $\sigma = \sigma_0 + a^2\sigma_1 + \cdots$.

### 5.2. *Linearized stability of the bifurcating solutions*

We now turn our attention to the determination of the stability characteristics of the small-amplitude bifurcated solution constructed above. Writing

$$(U_m, \Theta_m, V_0) = (U_0, \Theta_0, V_0) + \delta(U_1, \Theta_1, V_1) + \ldots,$$

where $0 < \delta \ll 1$, substituting into (3.18)-(3.20) and linearizing about the periodic solution $(U_0, \Theta_0, V_0)$ gives

$$\left.\begin{aligned}
\frac{\partial V_1}{\partial T_2} &= \frac{\partial^2 V_1}{\partial y^2} - (\alpha_1 - 2\mathrm{i}y^2)V_1 - \mathrm{i}(V_0 U_1 + U_0 V_1) - \frac{4}{3}\left(V_0\frac{\partial \Theta_1}{\partial y} + V_1\frac{\partial \Theta_0}{\partial Z}\right), \\
\frac{\partial U_1}{\partial T_2} &= \frac{\partial^2 U_1}{\partial y^2} - \mathrm{i}\left(V_1^*\frac{\partial^2 V_0}{\partial y^2} + V_0^*\frac{\partial^2 V_1}{\partial y^2} - V_1\frac{\partial^2 V_0^*}{\partial y^2} - V_0\frac{\partial^2 V_1^*}{\partial y^2}\right), \\
\frac{\partial \Theta_1}{\partial T_2} &= \frac{1}{2}\frac{\partial^2 \Theta_1}{\partial y^2} - \frac{\partial}{\partial y}\left(V_0 V_1^* + V_1 V_0^*\right),
\end{aligned}\right\} \tag{5.4}$$

which must be solved subject to the boundary conditions

$$V_1, U_1, \Theta_1 \to 0 \quad \text{as} \quad |y| \to \infty.$$

The coefficients appearing in (5.4) are $2\pi/\omega$-periodic in $T_2$, where $\omega$ is defined in §5.1, and hence on the basis of Floquet theory we look for solutions in the form

$$(V_1, U_1, \Theta_1) = (V_{11}, U_{11}, \Theta_{11})\mathrm{e}^{\gamma T_2}, \tag{5.5}$$

where the amplitudes $V_{11}, U_{11}$ and $\Theta_{11}$ are $2\pi$-periodic in $T = \omega T_2$ and the Floquet exponent $\gamma$ is to be determined. (We note that, owing to the presence of the $V_1$ and $V_1^*$ terms in (5.4), the Floquet exponent $\gamma$ is required to be real.)

Substituting (5.5) into (5.4) yields

$$\left.\begin{aligned}
\gamma V_{11} + \omega\frac{\partial V_{11}}{\partial T} &= \frac{\partial^2 V_{11}}{\partial y^2} \\
&\quad -(\alpha_1 - 2iy^2)V_{11} - i(V_0 U_{11} + U_0 V_{11}) - \frac{4}{3}\left(V_0\frac{\partial \Theta_{11}}{\partial y} + V_{11}\frac{\partial \Theta_0}{\partial y}\right), \\
\gamma U_{11} + \omega\frac{\partial U_{11}}{\partial T} &= \frac{\partial^2 U_{11}}{\partial y^2} - \mathrm{i}\left(V_{11}^*\frac{\partial^2 V_0}{\partial y^2} + V_0^*\frac{\partial^2 V_{11}}{\partial y^2} - V_{11}\frac{\partial^2 V_0^*}{\partial y^2} - V_0\frac{\partial^2 V_{11}^*}{\partial y^2}\right), \\
\gamma \Theta_{11} + \omega\frac{\partial \Theta_{11}}{\partial T} &= \frac{1}{2}\frac{\partial^2 \Theta_{11}}{\partial y^2} - \frac{\partial}{\partial y}\left(V_{11}^* V_0 + V_0^* V_{11}\right),
\end{aligned}\right\} \tag{5.6}$$

which must be solved subject to the requirement that the disturbances decay as $|y| \to \infty$. The system (5.6) then represents an eigenvalue problem for the Floquet exponent $\gamma$. In general this problem must be solved numerically; however in the small-amplitude limit (of the bifurcated solution) considerable analytic progress can be made in determining the leading-order behaviour of the Floquet exponent and hence the stability of the bifurcating solution. As the following analysis is standard, we give only a brief outline here; full details can be found in any standard text on bifurcation theory (see for example Iooss & Joseph 1980).

To proceed, we first recall that, in the small-amplitude limit, the bifurcated solution can be expanded as

$$(V_0, U_0, \Theta_0) = a(V_{00}, aU_{00}, a\Theta_{00}) + \cdots,$$

with the frequency and wavenumber of the bifurcated solution expanded as

$$(\omega, \alpha_1) = (\omega_0, \alpha_{00}) + a^2(\omega_2, \alpha_{11}) + \ldots,$$

where $V_{00}$ etc. were determined in §5.1. We now expand

$$(V_{11}, U_{11}, \Theta_{11}) = (\hat{V}_0, 0, 0) + a(\hat{V}_1, a\hat{U}_0, a\hat{\Theta}_0) + a^2(\hat{V}_2, a\hat{U}_2, a\hat{\Theta}_2) + \ldots,$$

and

$$\gamma = \gamma_0 + a\gamma_1 + a^2\gamma_2 + \cdots.$$

Substitution of these expressions into (5.6) and equating coefficients of $a$ to zero yields, at leading order,

$$\gamma_0\hat{V}_0 + \omega_0\frac{\partial \hat{V}_0}{\partial T} = \frac{\partial^2 \hat{V}_0}{\partial y^2} - (\alpha_{00} - 2\mathrm{i}y^2)\hat{V}_0, \tag{5.7}$$

$$\gamma_0\hat{U}_1 + \omega_0\frac{\partial \hat{U}_1}{\partial T} = \frac{\partial^2 \hat{U}_1}{\partial y^2} - \mathrm{i}\left(\hat{V}_0^*\frac{\partial^2 V_{00}}{\partial y^2} + V_{00}^*\frac{\partial^2 \hat{V}_0}{\partial y^2} - \hat{V}_0\frac{\partial^2 V_{00}^*}{\partial y^2} - V_{00}\frac{\partial^2 \hat{V}_0^*}{\partial y^2}\right), \tag{5.8}$$

$$\gamma_0\hat{\Theta}_1 + \omega_1\frac{\partial \hat{\Theta}_1}{\partial T} = \frac{1}{2}\frac{\partial^2 \hat{\Theta}_1}{\partial y^2} - \frac{\partial}{\partial y}\left(V_{00}\hat{V}_0^* + \hat{V}_0 V_{00}^*\right). \tag{5.9}$$

Consider first equation (5.7). Multiplying this equation by $A_0$, where $A_0$ is the leading-order term in the expansion for the bifurcated solution given by (4.7*a*), integrating from $-\infty$ to $\infty$ and imposing the condition that $\hat{V}_0$ be $2\pi$-periodic in $T$ yields the result that $\gamma_0 \equiv 0$. Furthermore the leading-order eigenfunction $\hat{V}_0$ can then be written as

$$\hat{V}_0 = \Delta_0 A_0 \mathrm{e}^{\mathrm{i}T}.$$

At next order we obtain an equation identical to (5.7), with $\gamma_0$ replaced by $\gamma_1$ and $\hat{V}_0$

replaced by $\hat{V}_1$. Again applying the Fredholm alternative condition and imposing the condition that $\hat{V}_1$ be $2\pi$-periodic in $T$ yields $\gamma_1 \equiv 0$ and $\hat{V}_1 = \Delta_1 A_0 e^{iT}$. As $\hat{V}_1$ is a linear multiple of $\hat{V}_0$ we can, without loss of generality, set $\Delta_1 \equiv 0$.

With $\gamma_0 = \gamma_1 = 0$ we then have, at third order in our expansion,

$$\omega_0 \frac{\partial \hat{V}_2}{\partial T} - \frac{\partial^2 \hat{V}_2}{\partial y^2} + (\alpha_{00} - 2iy^2)\hat{V}_2 = -(\gamma_2 + \alpha_{11})\hat{V}_0 - \omega_2 \frac{\partial \hat{V}_0}{\partial T} - iV_{00}\hat{U}_1 - iU_{00}\hat{V}_0 - \frac{4}{3}V_{00}\frac{\partial \hat{\Theta}_1}{\partial y} - \frac{4}{3}\hat{V}_0 \frac{\partial \Theta_0}{\partial y}. \tag{5.10}$$

At this juncture we note that $V_{00} = A_0 e^{iT}$ so that, from (5.8) and (5.9), we obtain

$$\hat{U}_1 = i(\Delta_0 + \Delta_0^*) \int_y^\infty \left( A_0 \frac{\partial A_0^*}{\partial z} - A_0^* \frac{\partial A_0}{\partial z} \right) dz, \qquad \frac{d\hat{\Theta}_1}{dy} = 2(\Delta_0 + \Delta_0^*)|A_0|^2, \tag{5.11}$$

where we have employed the fact that the only $2\pi$-periodic solutions of (5.8) and (5.9) are ones for which $\hat{U}_1$ and $\hat{\Theta}_1$ are steady. Also, from §5.1 we have

$$U_{00} = i \int_y^\infty \left( A_0 \frac{\partial A_0^*}{\partial z} - A_0^* \frac{\partial A_0}{\partial z} \right) dz, \qquad \frac{d\Theta_{00}}{dy} = 2|A_0|^2.$$

Turning our attention to (5.10), upon applying the Fredholm alternative condition and the constraint that $\hat{V}_2$ be $2\pi$-periodic in $T$, we obtain

$$-(\gamma_2 + \alpha_{11} + i\omega_2)\Delta_0 + \sigma_1(\Delta_0^* + 2\Delta_0) = 0, \tag{5.12}$$

where we have made use of the result, from §5.1, that

$$\sigma_1 = \alpha_{11} + i\omega_2 = \left[ \int_{-\infty}^\infty A_0^2 \left\{ \int_y^\infty \left( A_0 \frac{\partial A_0^*}{\partial z} - A_0^* \frac{\partial A_0}{\partial z} \right) dz \right\} dy - \frac{8}{3} \int_{-\infty}^\infty A_0^2 |A_0|^2 dz \right] \Big/ \int_{-\infty}^\infty A_0^2 \, dz.$$

Simplifying (5.12) yields

$$\gamma_2 \Delta_0 = \sigma_1(\Delta_0^* + \Delta_0).$$

Finally writing $\Delta_0 = re^{i\beta}$ and taking real and imaginary components yields

$$\gamma_2 = \frac{1}{\alpha_{11}}(\cos 2\beta + 1)(\alpha_{11}^2 + \omega_2^2), \tag{5.13}$$

where $\beta$ is determined from

$$(\cos 2\beta + 1)/\sin 2\beta = \alpha_{11}/\omega_2. \tag{5.14}$$

With the phase $\beta$ determined from (5.14) the Floquet exponent is then given by (5.13). In particular, we note from (5.14) that $\cos 2\beta + 1 > 0$ (since $\alpha_{11}$ and $\omega_2$ are both negative). Thus $\gamma_2 < 0$ for all modes of the bifurcated solutions. Hence, in the small-amplitude limit, the family of periodic solutions of the system (3.18)–(3.20) are stable and so at each of the successive critical points the system undergoes a supercritical Hopf bifurcation.

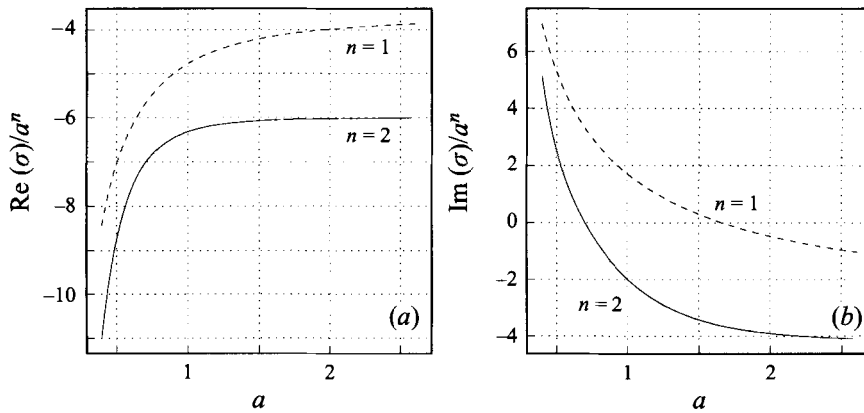


FIGURE 5. Plots of $\mathrm{Re}(\sigma)/a^n$ and $\mathrm{Im}(\sigma)/a^n$ versus amplitude $a$. Shown are mode 1 (solid line, $n = 2$), mode 2 (dashed line, $n = 1$).

## 6. The large-amplitude limit

With the small-amplitude analysis given above we may now turn our attention to the question of the limiting, large-amplitude, behaviour of the bifurcated solutions governed by equation (4.8). In figure 5 we present a plot of $a^{-n}\mathrm{Re}(\sigma)$ and $a^{-n}\mathrm{Im}(\sigma)$ versus the wave amplitude $a$, where $\sigma$ was determined in §4. Shown are results for the first two modes, mode 1 being even in $y$ whereas mode 2 is odd in $y$. This figure clearly demonstrates that two different asymptotic structures exist in the large-$a$ limit; in particular we have the result

$$\left.\begin{array}{lll} \sigma \sim \sigma_0 a^2 & \text{as} \quad a \to \infty & \text{(for even modes),} \\ \sigma \sim \sigma_0 a & \text{as} \quad a \to \infty & \text{(for odd modes).} \end{array}\right\} \tag{6.1}$$

We will therefore present the analysis of each asymptotic form separately.

### 6.1. *Even modes*

Turning our attention to the eigenfunction plots presented in figure 3(*a,b,e,f*) we readily observe that the eigenfunctions become increasingly localized about the position $y = 0$. This suggests that a new dominant normal length scale will emerge as the amplitude of the disturbance is further increased. By writing $z = a^n y$, substituting into (4.8) and considering a balance of normal diffusion with nonlinearity suggests that we choose $n = 1$ so that $z = ay$ and the mode is localized to an $O(a^{-1})$ layer situated at $y = 0$. With the dominant length and time scales of the disturbance determined we proceed by seeking solutions to equation (4.8) in the form

$$A = A_0(z) + a^{-1}A_1(z) + O(a^{-2}), \tag{6.2}$$

where

$$\sigma = a^2\left(\hat{\sigma}_0 + a^{-1}\hat{\sigma}_1 + O(a^{-2})\right). \tag{6.3}$$

Substitution of these expansions into equation (4.8) and equating reciprocal powers of $a$ to zero yields, at leading order

$$\frac{\mathrm{d}^2 A_0}{\mathrm{d}z^2} - \hat{\sigma}_0 A_0 + A_0 \int_0^\infty \left(A_0 \frac{\mathrm{d}A_0^*}{\mathrm{d}v} - A_0^* \frac{\mathrm{d}A_0}{\mathrm{d}v}\right) \mathrm{d}v - \tfrac{8}{3} A_0 |A_0|^2 = 0. \tag{6.4}$$

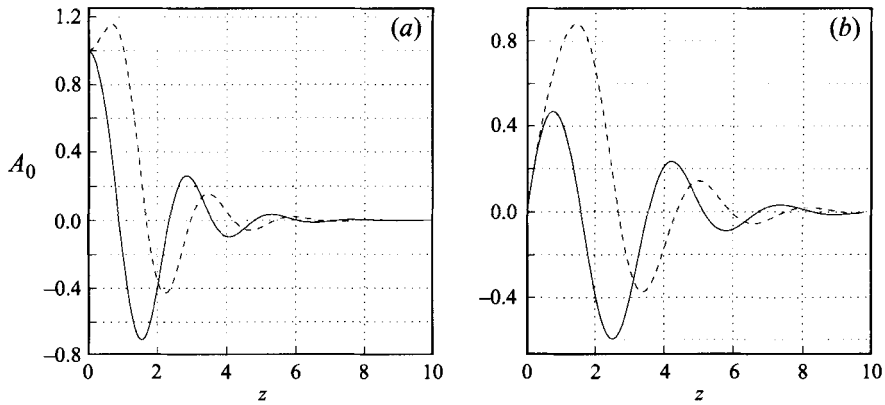


FIGURE 6. Plots of the limiting forms of the eigenfunctions. Shown are (*a*) the first even mode and (*b*) the first odd mode. Solid line: real component of the eigenfunction, dashed line imaginary component of the eigenfunction.

Similar, inhomogeneous versions of equation (6.4), governing the amplitude corrections $A_1$, $A_2$ etc. can readily be derived. However, as we are predominantly interested in the leading-order behaviour of the solution, in particular $\hat{\sigma}_0$, we will restrict our attention to (6.4). This equation must be solved subject to the boundary conditions

$$A_0 = 1 + \mathrm{i}, \quad \frac{\mathrm{d}A_0}{\mathrm{d}z} = 0 \quad \text{on} \quad z = 0, \qquad A \to 0 \quad \text{as} \quad z \to \infty. \tag{6.5}$$

The system (6.4), (6.5) was solved in a manner similar to that described in §4.1 for equation (4.8) with the result that the first modal solution was found with eigenvalue

$$\hat{\sigma}_0 = -6.0000 - 4.2164\mathrm{i}. \tag{6.6}$$

The corresponding eigenfunction is shown in figure 6. We note, from figure 5, that the agreement with (6.6) is good even down to $O(1)$ values of the wave amplitude.

### 6.2. *Odd modes*

Turning our attention to the odd modal solutions of (4.8) we note, from the eigenfunction plots presented in figure 3($c, d, g, h$) that the modes again become increasingly localized about $y = 0$ and, unlike the even modes discussed above, decrease in amplitude as the wave amplitude parameter $a$ is increased. Thus writing $z = a^m y$ and $A = a^r B$, substituting into (4.8) and again balancing normal diffusion with nonlinearity (noting of course that $\sigma = O(a)$ from (6.1)) we find $m = -r = 1/2$. Thus the odd modes become localized to within an $O(a^{-1/2})$ layer situated at $y = 0$ and, furthermore, their amplitude decreases like $a^{-1/2}$ as $a \to \infty$.

We may now proceed by seeking solutions to equation (4.8) in the form

$$A = a^{-1/2}\left(A_0(z) + a^{-1}A_1(z) + O(a^{-2})\right),$$

where

$$\sigma = a^{1/2}\left(\hat{\sigma}_0 + a^{-1}\hat{\sigma}_1 + O(a^{-2})\right),$$

and $z = a^{1/2}y$. Substituting these expressions into (4.8) we obtain, at leading order, an equation governing $A_0$ which is identical to (6.4), but with the modified boundary condition

$$A_0 = 0, \quad \frac{\mathrm{d}A_0}{\mathrm{d}z} = 1 + \mathrm{i} \quad \text{on} \quad z = 0, \qquad A \to 0 \quad \text{as} \quad z \to \infty. \tag{6.7}$$

Solving (6.4) with the boundary condition (6.7) gives, for the first eigenvalue,

$$\hat{\sigma}_0 = -3.6555 - 2.4493\mathrm{i}.$$

Comparison with figure 5 shows reasonable agreement for $O(1)$ values of $a$; this agreement would improve if the results of figure 5 were taken to higher wave amplitudes. The corresponding first odd eigenfunction is shown in figure 6.

Thus, in the large-amplitude limit, a new structure emerges in which the wave motion becomes increasingly localized about the position at which the streamwise velocity attains its maximum value. Additionally, it is the modes which are symmetric about this position that dominate the flow. The asymmetric modes decrease in amplitude and become increasingly less important in determining the large-amplitude response of the flow. The decrease in wavenumber and frequency of the finite-amplitude wave motions, as evidenced by (3.5) and (6.3), suggests that a new dominant structure will emerge as the wavenumber of the disturbance is taken further into the régime where linear theory predicts instability.

It is a relatively simple matter to determine the next distinguished limit in the current asymptotic expansion. Thus, with the knowledge that $\sigma = O(a^2)$ as $a \to \infty$, and in particular $\alpha_{01} = O(a^2)$, we then find that the expansion of the wavenumber, given by (3.5), becomes disordered when the wave amplitude $a = O(Re^{1/16})$. New dominant time and length scales will then emerge in this strongly nonlinear limit. It is then a simple matter to describe the equations appropriate to this large-amplitude limit. An analysis of the governing equations in this new distinguished limit is currently under way and we hope to report on this work in the near future (see Mureithi 1996).

## 7. Conclusions

We have demonstrated the existence of a family of finite-amplitude periodic solutions to the Navier–Stokes equations governing the boundary layer flow over a strongly heated flat plate. The controlling factor, in regard to the boundary layer flow, for such solutions to exist is that the streamwise velocity overshoot its (normalized) free-stream value somewhere within the boundary layer. Such overshooting is readily shown to occur in boundary layers which are strongly thermally stratified; strong in the sense that the momentum and temperature fields within the boundary layer are fully coupled.

The finite-amplitude periodic solutions which can exist are found in regions of the parameter space where linear theory predicts instability. Thus the flow undergoes a supercritical Hopf bifurcation as the point of linear, neutral stability is crossed. These finite-amplitude periodic solutions are described by a novel mean flow/first harmonic interaction theory in which the wave and the wave-induced mean flow are of comparable size. As such the motions we have described are strongly weakly nonlinear and cannot be developed through a standard Stuart–Landau amplitude equation approach to weakly nonlinear theory. Furthermore, the structures we have described suggest the existence of a new, larger amplitude, family of periodic solutions to the full Navier-Stokes equations. This new asymptotic régime is currently under investigation and we hope to report our findings in the near future.

The analysis described above is readily extended, with suitable modifications, to a large variety of physically important flows of which heated Poiseuille and Poiseuille–Couette flow are two examples. Thus, in both external and internal buoyancy-driven flows it is possible for stable nonlinear wave motions to exist within a thin region away

from any bounding surface. We have described a mechanism by which convection roll cells can be localized at the position where the streamwise velocity attains its maximum. Of course, other instability mechanisms are operable within the mixed forced–free convection boundary layers consider here, longitudinal vortex instabilities being one such example (see Hall 1993). However, the wave motions described here have much larger growth rates than the vortex-like instabilities and as such we would expect the wave-like instabilities, and the nonlinear wave motions described here, to dominate the flow. Such a conjecture can only be tested by a direct numerical simulation of forced–free convection boundary layers.

The work of E.W.M. was supported by an AIDAB Scholarship. The work of J.P.D. was supported by the Australian Research Council through their small grant scheme. We would like to thank Dr P. Blennerhassett for several useful comments regarding the numerical solution of equations (4.8) and (6.4). We would like to thank the anonymous referees whose comments helped to improve the presentation of this paper.

## REFERENCES

ABRAMOWITZ, M. & STEGUN, I.A. 1965 *Handbook of Mathematical Functions*. Dover.

BASSOM. A. P. & HALL, P. 1989 On the generation of mean flows by the interaction of Görtler vortices and Tollmien–Schlichting waves in curved channel flows. *Stud. Appl. Maths* **81**, 185.

BENNEY, D. J. & CHOW, K. 1985 An alternative approach to nonlinear instabilities in hydrodynamics. *Stud. Appl. Maths* **73**, 261–267.

BENNEY, D. J. & CHOW, K. 1986 Instabilities of waves on a fee surface. *Stud. Appl. Maths* **74**, 227–243.

BENNEY, D. J. & CHOW, K. 1989 A mean flow first harmonic theory for hydrodynamic stability. *Stud. Appl. Maths* **80**, 37–73.

BODONYI, R. J. & SMITH, F. T. 1981 The upper branch stability of the Blasius boundary layer, including non-parallel flow effects. *Proc. R. Soc. Lond.* A **375**, 65–92.

DENIER, J. P. 1992 The development of fully nonlinear Taylor vortices. *IMA J. Appl. Maths* **49**, 15–33.

DRAZIN, P. G. & REID, W. H. 1981 *Hydrodynamic Stability*. Cambridge University Press.

GAGE, K. S. 1971 The effect of stable thermal stratification on the stability of viscous parallel flows. *J. Fluid Mech.* **47**, 1–20.

GAGE, K. S. & REID, W. H. 1968 The stability of thermally stratified plane Poiseuille flow. *J. Fluid Mech.* **33**, 21–32.

HALL, P. 1982 Taylor–Görtler vortices in fully developed or boundary layer flows: linear theory. *J. Fluid Mech.* **124**, 475–494.

HALL, P. 1983 On the non-linear evolution of Görtler vortices in non-parallel boundary layers. *IMA J. Appl. Maths* **29**, 173–196.

HALL, P. 1990 Görtler vortices in growing boundary layers: the leading edge receptivity problem, linear growth and the nonlinear breakdown stage. *Mathematika* **37**, 151–189.

HALL, P. 1993 Streamwise vortices in heated boundary layers. *J. Fluid Mech.* **252**, 301–324.

HALL, P. & LAKIN, W. D. 1988 The fully nonlinear development of Görtler vortices in growing boundary layers. *Proc. R. Soc. Lond.* A **415**, 421–444.

HALL, P. & MORRIS, H. 1992 On the instability of boundary layers on the heated flat plates. *J. Fluid Mech.* **245**, 367–400.

IOOSS, G. & JOSEPH, D. D. 1980 *Elementary Stability and Bifurcation Theory*. Springer.

LIN, C. C. 1955 *The Theory of Hydrodynamic Stability*. Cambridge University Press.

MUREITHI, E. W. 1996 The effect of thermal stratification on the stability properties of boundary layer flows. PhD Thesis, University of New South Wales.

MUREITHI, E. W. & DENIER, J. P. 1996 The effect of buoyancy on lower branch Tollmien–Schlichting waves: weakly nonlinear theory (in preparation).

MUREITHI, E. W., DENIER, J. P. & STOTT, J. A. K. 1996 The effect of buoyancy on upper branch Tollmien–Schlichting waves. *IMA J. Appl. Maths* (submitted).

REID, W.H. 1965 The stability of parallel flows. In *Basic Developments in Fluid Dynamics*, vol. 1 (ed. M. Holt), pp. 249–307. Academic.

SEDDOUGUI, S. O., BOWLES, R. I. & SMITH, F. T. 1981 Surface-cooling effects on compressible boundary-layer instability, and on upstream influence. *Eur. J. Mech.* B/*Fluids* **10**, 117–145.

SMITH, F. T. 1979*a* On the non-parallel flow stability of the Blasius boundary layer. *Proc. R. Soc. Lond.* A **366**, 91–109.

SMITH, F. T. 1979*b* Nonlinear stability of boundary layers for disturbances of various sizes. *Proc. R. Soc. Lond.* A **368**, 573–589.

SMITH, F. T. & BODONYI, R. J. 1980 On the stability of the developing flow in a channel or circular pipe. *Q. J. Mech. Appl. Maths* **33**, 293–320.

SMITH, F. T. & BODONYI, R. J. 1982 Nonlinear critical layers and their development in streaming-flow stability. *J. Fluid Mech.* **118**, 165–185.

STEWARTSON, K. 1964 *The Theory of Laminar Boundary Layers in Compressible Fluids*. Clarendon.

STREHLE, E. 1978 Stabilitätsberechnung dichtegeschichteter ebener Wandgrenzschichten. *Z. Angew. Math. Mech.* **58**, 539–552.

STUART, J. T. 1963 Hydrodynamic stability. In *Laminar Boundary Layers* (ed. L. Rosenhead). Clarendon Press.